BIOCHEMISTRY
including biophysical chemistry & molecular biology

Article

pubs.acs.org/biochemistry

What's in Your Buffer? Solute Altered Millisecond Motions Detected by Solution NMR

Madeline Wong,[†,§] Gennady Khirich,[†] and J. Patrick Loria*[,†,‡]

[†]Department of Chemistry and [‡]Department of Molecular Biophysics and Biochemistry, Yale University, New Haven, Connecticut 06520, United States

Supporting Information

ABSTRACT: To date, little work has been conducted on the relationship between solute and buffer molecules and conformational exchange motion in enzymes. This study uses solution NMR to examine the effects of phosphate, sulfate, and acetate in comparison to MES- and HEPES-buffered references on the chemical shift perturbation and millisecond, chemical, or conformational exchange motions in the enzyme ribonuclease A (RNase A), triosephosphate isomerase (TIM) and HisF. The results indicate that addition of these solutes has a small effect on ^{1}H and ^{15}N chemical shifts for RNase A and TIM but a significant effect for HisF. For RNase A and TIM, Carr−Purcell−Meiboom−Gill relaxation dispersion experiments, however, show significant solute-dependent changes in conformational exchange motions. Some residues show loss of millisecond motions relative to the reference sample upon addition of solute, whereas others experience an enhancement. Comparison of exchange parameters obtained from fits of dispersion data indicates changes in either or both equilibrium populations and chemical shifts between conformations. Furthermore, the exchange kinetics are altered in many cases. The results demonstrate that common solute molecules can alter observed enzyme millisecond motions and play a more active role than what is routinely believed.

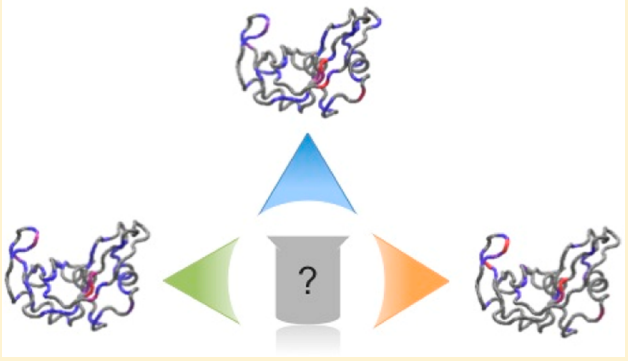

In 1930, Mann and Woolf[1] showed that sulfate inhibited the enzymatic conversion of fumaric acid to L-malic acid. Subsequently, it was shown that phosphate, as well as common buffer components, could act both as an inhibitor and activator of fumarase activity.[2,3] That revealing work demonstrated that buffers and solutes could bind to enzymes and alter properties of their catalytic behavior including K_m and V_m values. That buffers could play a more active and often undesirable role was described for Tris (tris[hydroxymethyl] aminomethane) buffer, where the amine-containing buffer could act as an enzymatic substrate, inhibitor, and activator or form complexes with substrate.[4] More recently as found in the Protein Data Bank (PDB), small molecule solutes have been identified by X-ray crystallography at the active sites as well as other locations in proteins.[5] Because these small molecules can alter the enzyme function either directly through competitive binding or indirectly via structural alterations at allosteric sites, it raises the question of whether buffer components can also alter or induce conformational motions in enzymes.

Given the increasing number of studies of functional protein motions, we sought to investigate this question by analyzing the effects of buffer and solute on the millisecond (ms) conformational exchange motions in three enzymes. Previous work in our lab showed that RNase A possesses millisecond motions that are crucial to its function.[6−12] Early in that work, we decided against using phosphate or acetate buffers because the latter was observed in the active site in one crystal structure and because we reasoned the former would bind to RNase A given the enzyme's job of binding and cleaving RNA, a phosphate polymer. Similar observations were made for sulfate. Prior to detailed NMR studies, we verified that RNase A in MES buffer at pH = 6.4 and in unbuffered solution at the same pH exhibited identical millisecond motions, confirming MES as a pH buffer and nothing more.[7] Here, we reinvestigate these issues by measuring millisecond motions in RNase A in the presence of phosphate, sulfate, and acetate and comparing these to those of a MES-buffered reference. Structural and thermodynamical evidence suggested that these small anions interacted with RNase A.

A number of anions stabilize RNase A from urea denaturation, demonstrating a reduction in the denaturation rate constant of 66%, 42%, and 29% for solutions of sulfate, acetate, and chloride, respectively; the postulated mechanism involves a single anion binding to the enzyme active site.[13] Berisio et al. deduced the importance of the P2 phosphate-binding site, which "induces an enhanced catalytic efficiency", from atomic resolution structures and site-directed mutagenesis of RNase A.[14] The group also noted that a sulfate ion, an analogue for the phosphate group of RNA, binds in the active

Received: July 22, 2013
Revised: August 14, 2013
Published: August 30, 2013

site to the catalytic residues His12, His119, and Lys41. At neutral pH, ion release correlates with uptake of water molecules and conformation changes in the pH-dependent active-site residues Lys41 and Gln11. It is postulated that these tertiary structure changes result from pH effects on electrostatic potential, which may produce enzyme closure and sulfate anion release at high pH.[14] Other studies have noted the influence of phosphate and acetate on His48 proton transfer, as well as changes in pK_a values of adjacent histidine residues; weak bases such as sulfate and chloride result in a slower proton exchange rate, though 0.08 M sulfate shifts His12 and His119 pK_a values by ∼0.4 units.[15,16]

Though both the pH dependence of the atomic resolution structures and solution NMR experiments have been performed, to date there has been little work on the effect of solutes or buffer molecules on enzyme dynamics. RNase A has been known to weakly bind small ionic molecules such as acetate, formate, phosphate, and sulfate, which may be present in experimental buffer conditions.[16] But Mueller-Dieckmann et al. observed that for >90% of anomalously scattering substructures (23 crystal structures of 19 biological macromolecules) examined with atomic resolution of 2.0 Å, "chloride, sulfate, phosphate or metal ions from the buffer or even from the purification protocol are frequently bound to the protein molecule and that these ions are often overlooked, especially if they are not bound at full occupancy".[17] In contrast, those authors' analysis of the Protein Data Bank indicated that only about 32% of reported protein structures have bound phosphate, sulfate, chloride, potassium, or calcium ions (and this number may be an overestimate because it does not omit cases where two or more different ions are bound).

Like RNase A, motions of the TIM active site loop (loop 6) are known to be integral to its catalytic function.[18−23] TIM catalyzes the isomerization of a pair of phosphate containing trioses and a crystal structure (PDB ID: 8TIM) shows electron density for sulfate at the active site. Thus, it seems reasonable to also expect anionic buffer molecules to bind to TIM and potentially alter conformational motions.

The enzyme HisF is a 253 amino acid monomer that comprises one-half of the imidazole glycerol phosphate synthase (IGPS) heterodimer. The two catalytic subunits in IGPS are HisH and HisF, with HisH catalyzing the production of ammonia from the hydrolysis of glutamine followed by the HisF-catalyzed cleavage and cyclization of *N*′-[(5′-phosphoribulosyl)formimino]-5-aminoimidazole-4-carboxamide-ribonucleotide (PRFAR) with NH_3 to produce imidazole glycerol phosphate (IGP) and 5-aminoimidazole-4-carboxamide ribotide (AICAR). As with TIM and RNase A, an X-ray crystal structure of HisF shows the presence of phosphate ions at the active site, again suggesting that anionic buffers or small molecules could alter the conformational motions in this enzyme.

To investigate these possibilities, we examined the chemical shifts and dynamics of RNase A, TIM, and HisF in a variety of buffers at identical pH and ionic strengths. The results of these studies suggest that the effect of phosphate, sulfate, and acetate ions or potentially many other commonly used solutes on enzyme dynamics, under common experimental conditions, merits closer examination. Here, we conducted a set of solution NMR experiments to investigate the chemical shift perturbation effected by these different buffer components; additionally, relaxation compensated Carr−Purcell−Meiboom−Gill dispersion (rcCPMG) experiments[24] were conducted under identical conditions to elucidate small molecule effects on millisecond enzyme motions. The results demonstrate that these molecules play a more active role than what is routinely believed.

MATERIALS AND METHODS

NMR Sample Preparation. A 400 μM ^{15}N-labeled sample of WT RNase A was prepared for study in either 100 mM sodium phosphate, 80 mM sodium sulfate, or 100 mM sodium acetate each with 0.01% NaN_3, 5% D_2O, 1% w/v DSS. For comparison, a reference RNase A sample was prepared in 5 mM MES−NaOH, 7 mM NaCl, 0.01% NaN_3, 5% D_2O, 1% w/v DSS, pH = 6.4.[7] In all cases, dialysis was performed overnight with 4 L of buffer using a 10K MWCO, 3−12 mL Slide-A-Lyzer Dialysis Cassette (Thermo Scientific).

An 850 μM ^{15}N,^{2}H isotopically labeled chicken triosephosphate isomerase (TIM) V167P/W168E double mutant was prepared in 10 mM MES, 10 mM NaCl, 7.5% D_2O at pH = 6.40 or a 10 mM sodium phosphate, 10 mM NaCl, 7.5% D_2O solution at pH = 6.40. The pH of both MES and phosphate solutions were adjusted with 1 M NaOH.

A third enzyme sample was prepared that contained 300 μM HisF monomer from the heterodimer enzyme imidazole glycerol phosphate synthase (IGPS) from *Thermotoga maritima*. The HisF sample was ^{15}N,^{2}H isotopically labeled and studied in 10 mM HEPES, 1 mM EDTA, 1 mM DTT, 7.5% D_2O at pH = 7.20 and 10 mM potassium phosphate, 1 mM EDTA, 1 mM DTT, 7.5% D_2O at pH = 7.20. The pH of both HEPES and phosphate solutions were adjusted with 1 M KOH.

Solution NMR Experiments. NMR experiments for all three enzymes were performed at 298 K as calibrated with a standard methanol sample on Varian/Agilent NMR spectrometers equipped with triple-resonance probes and pulsed-field gradients. Heteronuclear single-quantum coherence (HSQC) and standard ^{15}N-rcCPMG experiments were conducted at static magnetic fields of 14.1T for RNase A and HisF, whereas TROSY-based CPMG dispersion experiments[25] were performed at 18.8T for TIM, according to established pulse sequences. The ^{1}H carrier frequency was set to the water resonance, and the ^{15}N carrier frequency was set to 120 ppm. Spectra of RNase A, TIM, and HisF were typically acquired with (128 × 4096, 128 × 2194, 128 × 1280) complex points and spectral widths of 2640 × 10246, 2900 × 11000, 2200 × 10000 Hz in the (t1 × t2) dimensions, respectively. HSQC spectra were phase-corrected and processed with Varian and NMRDraw software (http://spin.niddk.nih.gov/NMRPipe/); peak assignments were correlated in Sparky (http://www.cgl.ucsf.edu/home/sparky/) from an assigned reference spectrum of MES-buffered WT RNase A,[7] MES-buffered TIM[26] and phosphate-buffered HisF.[27] CPMG spectra were processed with existing scripts (developed in-house) and NMRDraw software, and dispersion data were fit with the fast-exchange equation[28]

$$R_2(1/\tau_{cp}) = R_2^0 + \phi_{ex}/k_{ex}[1 - 2\tanh(k_{ex}\tau_{cp}/2)/(k_{ex}\tau_{cp})] \quad (1)$$

where $\phi_{ex} = p_a p_b \Delta\omega^2$ (with p_A and p_B as equilibrium populations of the interconverting conformers A and B and $\Delta\omega$ denoting the chemical shift difference between these two conformations), k_{ex} is the exchange rate constant and is the sum of the forward and reverse rate constants, R_2^0 is the "exchange-free" transverse relaxation rate, and τ_{cp} is the time delay between 180° CPMG pulses during the nitrogen relaxation period, with values of 0.625, 0.714 (×2), 1.0, 1.25, 1.67, 2.0,

dx.doi.org/10.1021/bi400973e | *Biochemistry* 2013, 52, 6548−6558

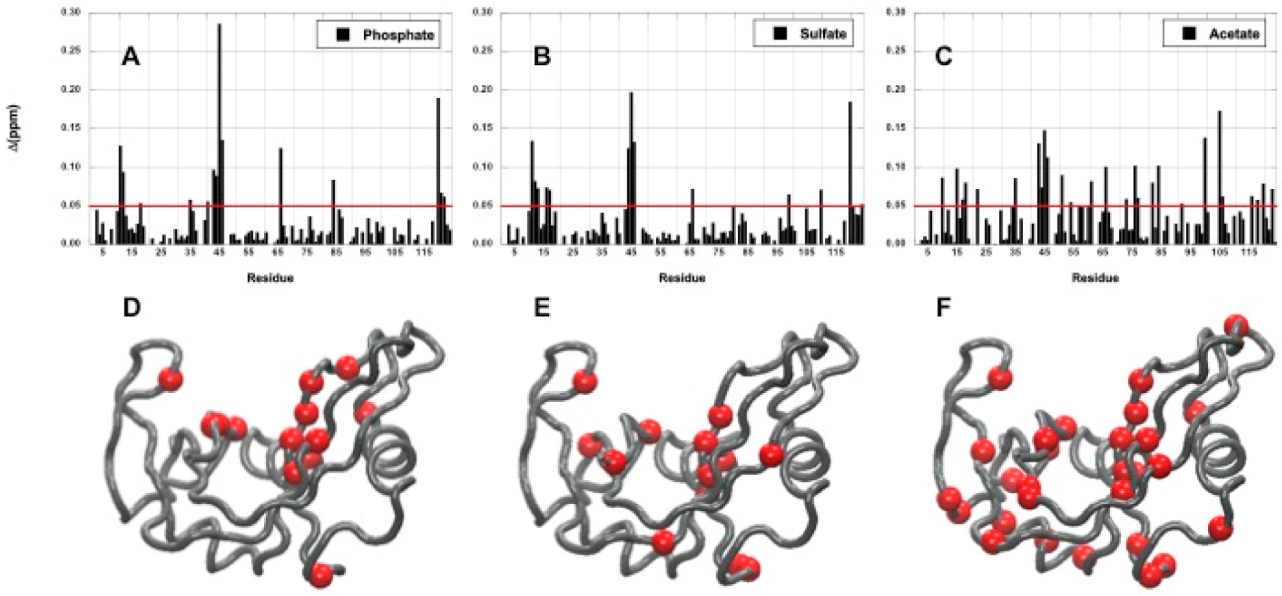

Figure 1. Chemical shift perturbations caused by phosphate (A, D), sulfate (B, E), and acetate (C, F). Composite $^{1}H,^{15}N$ chemical shifts (Δ) are shown on a per-residue basis (A–C). Residues with Δ values >0.05 ppm, given by the horizontal red line, are mapped onto the RNase A structure as red spheres (D–F). Δ was calculated as described by eq 3

2.50 (×2), 3.33, and 5.0 ms. $R_2(1/\tau_{cp})$ values were determined at each τ_{cp} relaxation time using the two-point constant time method[29] with total relaxation delays of 0 and 40 ms for RNase A and HisF, whereas a total CPMG relaxation time of 20 ms was used for TIM. To assess differences in k_{ex} values from the CPMG dispersion data, we used 50 Monte Carlo simulations for each buffer condition and each residue using experimentally determined uncertainties. We then compared the 50 resulting k_{ex} values for each buffer against those of the MES reference using an unpaired t test with $\alpha = 0.05$ to determine if the two distributions of k_{ex} values were statistically different.

R_{ex} values from relaxation dispersion fitting were also used to assess deviations from MES-reference conditions, where R_{ex} is defined as

$$R_{ex} = \phi_{ex}/k_{ex} \quad (2)$$

For chemical shift comparisons, all spectra were aligned to the reference spectrum using the proton shift of DSS at 0 ppm. Chemical shift perturbations were calculated for all HSQC spectra on the basis of the weighted chemical shift change per residue, Δ, defined as

$$\Delta = [(\Delta\delta(H^N)^2 + (\Delta\delta(N)^2/25))/2]^{1/2} \quad (3)$$

where $\Delta\delta(H^N)$ and $\Delta\delta(N)$ are measured changes in chemical shift for $^{1}H^{N}$ and ^{15}N, respectively, measured in parts per million.[30]

RESULTS

RNase A. Addition of phosphate, sulfate, or acetate has a small effect on the $^{1}H-^{15}N$ chemical shifts (Figure 1). Relative to the MES-buffered reference spectrum, the mean ± standard deviation of the chemical shift changes (Δ) are 0.03 ± 0.04, 0.03 ± 0.04, and 0.04 ± 0.04 ppm for phosphate, sulfate, and acetate, respectively. Phosphate and sulfate each result in 13 residues with Δ > 0.05 ppm, whereas significantly more (28 residues) surpass Δ > 0.05 when acetate is present, suggesting that RNase A is more sensitive to acetate than it is to either phosphate or sulfate. For comparison, binding of the product analogs 3′-cytidine monophosphate and 3′-thymidine monophosphate to RNase A results in mean Δ values >0.2 ppm with several residues having Δ > 0.5 ppm.[31] Despite the significant number of residues that experience chemical shift changes, the magnitude of these changes are rather small (almost 10-fold smaller) when compared to changes induced by ligands that resemble substrate or product.[6,9,31,32] Individual ^{1}H and ^{15}N chemical shift changes are shown in Supporting Information Figure S1. The results of these data show the same pattern as the composite shifts depicted in Figure 1, namely small shift changes due to buffer composition, with the largest changes coming from sites identified as anion binding sites.

For phosphate, chemical shift perturbed residues Gln11, His12, Lys41, Val43, and Asp121 all line the phosphate 1 (P1) binding subsite that interacts with the phosphate backbone in the binding of native RNA (Figure 1A,D).[33] Likewise, Lys66 forms the P0 pocket, and its amide chemical shifts are also altered by phosphate relative to the MES-buffered reference chemical shifts. Amino acid residues with significantly perturbed sulfate induced shifts include P0 residue Lys66 as well as P1 residues Gln11 and His12 (Figure 1B,E). Phe46 and Phe120 (near P1) as well as the β-strand (β1) residue Thr45, located near Lys41, also have significant shifts due to the presence of sulfate. Acetate, on the other hand, elicits a much wider distribution of residues with perturbed chemical shifts: Ser15 (loop 1) is located near His48, Lys66 is in the P0 pocket, and Val43 and Thr45 in β1 are near the P1 subsite and make important interactions with substrate, whereas Leu51 (α3), Tyr76, Cys84, Thr100 (β-hairpin 2), and His105 are more removed from active residues (Figure 1C,F). However, with the exception of Leu51 and Tyr76, nearly all residues perturbed by acetate are catalytically important (Arg10, Val43, Thr45, Phe46, Lys66), identified as involved in rate-limiting motions (Ser15, Thr17, Ser18, Ser22, Thr82, Thr100), or are adjacent to a key residue (Cys84, Asn44, Ser123). Interestingly, all three of the solutes alter the chemical shifts of loop 1, which is nearly 20 Å

dx.doi.org/10.1021/bi400973e | Biochemistry 2013, 52, 6548–6558

from the RNase A active site. The flexibility of this loop is crucial for the proper function of RNase A.[6,7]

Millisecond motions are essential for the function of RNase A. To determine solute effects on these motions, we first measured the transverse relaxation rate at the fastest pulsing frequency (R_2 @ τ_{cp} = 0.625 ms) in a CPMG dispersion experiment. The data is presented in Figure 2. The protein-

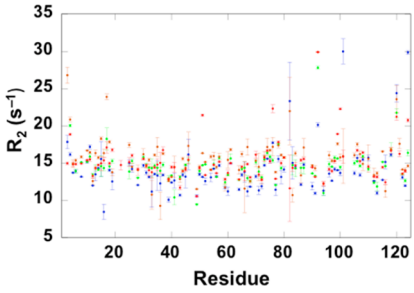

Figure 2. Transverse relaxation rate constants for RNase A. The R_2 values with τ_{cp} = 0.625 ms are shown for the reference (red), phosphate (green), sulfate (blue), and acetate (brown) samples.

wide mean values (±standard deviation) are very similar for the four solution conditions: R_2 = 15.2 ± 2.6, 14.6 ± 2.3, 14.0 ± 3.7, and 15.7 ± 3.1 s^{-1} for the reference, phosphate, sulfate, and acetate samples, respectively. However, it is clear from the data presented in Figure 2 that there are residue-specific differences in the R_2 values that depend on the solution in which RNase A is dissolved.

The differences in R_2 values observed between the reference sample and the phosphate, sulfate, and acetate samples indicate differences in protein motions. In some cases these differences in R_2 may be due to changes in picosecond−nanosecond motions, but we do not consider this further in the present study. Transverse relaxation rate constants are often used as a gauge of microsecond−millisecond motions, which in this case may include intra or intermolecular motions. Therefore, we next investigated what effect the different solutes would have on RNase A conformational exchange motions by performing ^{15}N CPMG relaxation dispersion experiments for each and comparing the results to those obtained for the MES reference standard. Somewhat surprisingly, there were clear differences in the dispersion curves between samples (Figure 3 and Supporting Information). In some cases, all solution conditions yielded identical data either showing no millisecond motions (Ala122) or the same millisecond motions (Asn71) as shown in Figure 3. However, as shown for Ala4, Ala19, Asp83, and Phe46, different dispersion data is obtained that depends on the solute. For Ala4, the reference sample shows millisecond motions, but no motions are observed for phosphate, sulfate, and acetate samples. For Ala19, Asp83, and Phe46, varying degrees of motion are observed that depend on solute. In some extreme cases like Ala19, it is clear that there is little observed motion for the reference or acetate samples, yet significant dispersion curves are observed for the phosphate and sulfate samples. In the case of Ala4 and Ala19, the R_2^0 values are

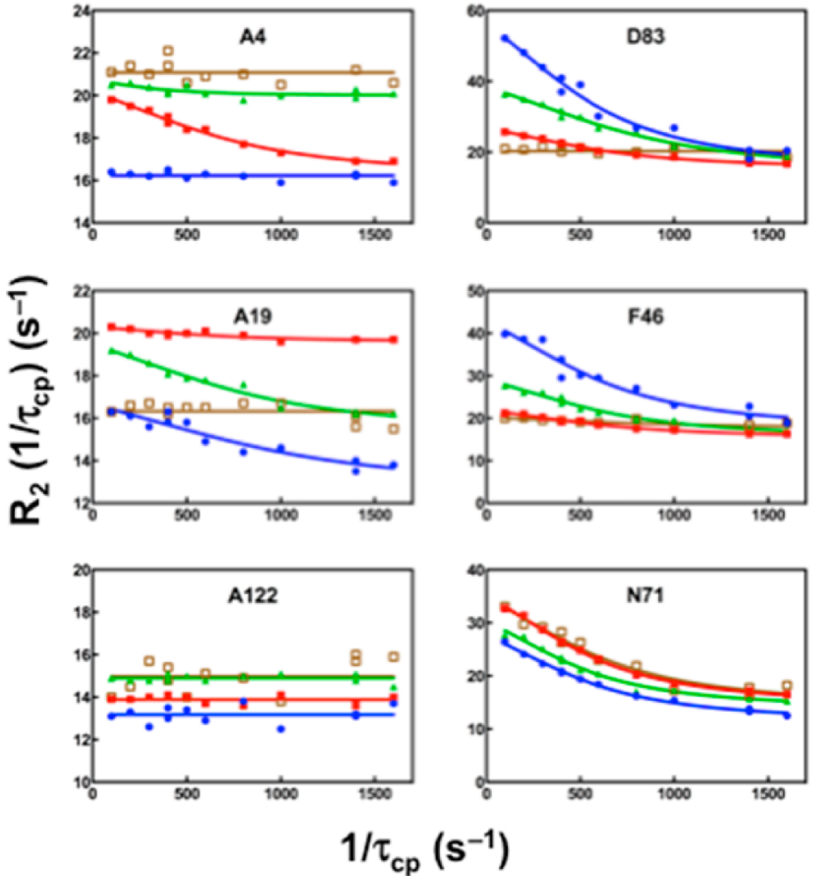

Figure 3. ^{15}N-CPMG dispersion curves. Data for MES reference (red), phosphate (green), sulfate (blue), and acetate (brown) are shown for select residues as indicated at the top of each graph.

dx.doi.org/10.1021/bi400973e | Biochemistry 2013, 52, 6548−6558

elevated by 4 and 6 s^{-1} for acetate and MES samples, respectively, versus the other buffer conditions. This increase likely reflects an increase in conformational motions into the high ms/low μs regime such that the effective field generated by CPMG pulses is ineffective at suppressing the exchange contribution to R_2. In cases such as this, it is possible that an $R_{1\rho}$ experiment may yield better results. Because only a small number of residues showed this type of behavior, we did not pursue this further.

For all quantifiable residues, we examined the amplitude of the dispersion curve, R_{ex}, as a semiquantitative indicator of millisecond motions as shown by eq 2. Figure 4 shows R_{ex}

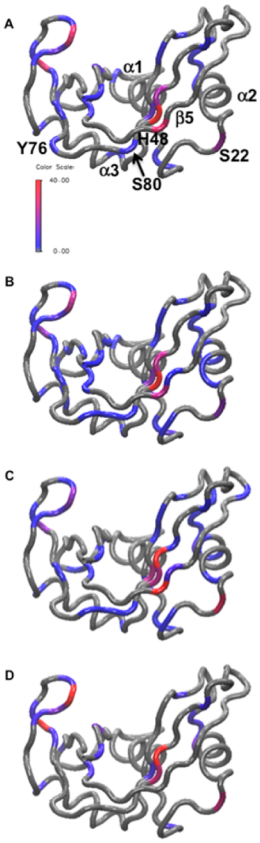

Figure 4. Millisecond motions in RNase A. Amino acid residues with R_{ex} ranging from zero (gray) to 40 s^{-1} (red, see color bar) are shown on a ribbon diagram of RNase A for MES reference (A), phosphate (B), sulfate (C), and acetate (D).

values mapped onto the backbone structure of RNase A. There are differences in R_{ex} magnitude between each solute and differences from the reference RNase A sample as indicated by the color gradient in Figure 4. Moreover, in some cases, an R_{ex} value is observed for one of the solute samples when no R_{ex} is seen in the reference, for example, α-helix 2 in the phosphate and sulfate samples (Figure 4B,C) versus this region in the reference (Figure 4A). Similarly, R_{ex} for the coil-like region between residues 76 and 80 is absent in the acetate sample, whereas this region has elevated R_{ex} in the center of the coil for phosphate and sulfate but on the ends of the coil for the reference enzyme (Figure 4).

Figure 5 shows these differences in more detail. Residues in which R_{ex} in the solute samples differs by more than 20% from the reference enzyme are shown in the graphs and mapped onto the structure. Blue regions in Figure 5D−F indicate the presence of motions that are absent in the reference sample, whereas red spheres indicate motions present in the reference that go undetected when phosphate, sulfate, or acetate are dissolved in the enzyme solution. These data show the significant differences in conformational exchange motions as they occur throughout the RNase A structure.

These differences in NMR-detected motions prompted us to compare the exchange parameters obtained from fits of the dispersion data to eq 1. At this temperature, nearly all of the MES-reference motions are in the fast limit, justifying the use of this simplified equation. The results of this comparison are shown in Figure 6, in which we compare the fit parameters k_{ex} and ϕ_{ex} for only those data in which notable dispersion data was obtained with $R_{ex} > 2$ s^{-1}. This comparison is limited to residues that show dispersion in the respective solution, to avoid having a number of data points at 0 for residues with flat dispersion curves. For completeness, dispersion data for all residues is shown in the Supporting Information (Figure S2).

In Figure 6 A−C and Table 1, a comparison of the kinetics of conformational motion is shown. It is clear that there are very few residues that have the same k_{ex} value in the various solutions compared to that of the MES reference. To illustrate the differences, for each residue, we compare the k_{ex} values obtained for phosphate, sulfate, and acetate with the MES reference sample. A perfect agreement between fit values would give a tight cluster (high correlation) on a line with unit slope. The correlation coefficient for the line of slope 1 is 0.69, 0.36, and 0.79 for the phosphate, sulfate, and acetate samples, respectively. The reference and phosphate samples share 17 residues with reasonable quality dispersion data. From these data, the mean k_{ex} values are 1883 s^{-1} for the MES sample and 1804 s^{-1} for the phosphate sample with an average pairwise difference in k_{ex} values of 426 s^{-1} and a standard deviation of 378 s^{-1}. Comparison of global fit parameters was not viable due to a lack of a conserved set of globally concerted residues under the different buffer conditions. A list of all residues used in this comparison is given in Table 1. A comparison of the 16 common residues between the reference and sulfate sample yielded mean values of 1978 s^{-1} for the MES sample and 1772 s^{-1} for the sulfate sample, with an average pairwise difference in k_{ex} values of 481 s^{-1} and a standard deviation of 325 s^{-1}. Lastly, a comparison of the exchange rate constants of the nine common residues for MES and acetate-containing samples gives mean k_{ex} = 1933 and 1735 s^{-1}, respectively, with a mean pairwise difference ± standard deviation =373 ± 268 s^{-1}. Thus, for each sample, there is an average difference of 20% in k_{ex} values from the MES reference sample, with some individual differences exceeding 80% of the reference.

Moreover, significant differences are also found in the ϕ_{ex} values determined from dispersion fitting (Figure 6 D−F). The linear correlation coefficients for phosphate, sulfate, and acetate with the reference are 0.47, 0.38, and 0.65 respectively. Because $\phi_{ex} = p_a p_b \Delta\omega^2$, these differences from the reference indicate changes in either or both equilibrium populations and chemical shifts between conformations.

Triosephosphate Isomerase. Buffer-induced changes in chemical shifts and NMR relaxation rates are not restricted to RNase A. The mean, 10%-trimmed chemical shift changes for TIM between MES and phosphate buffers at pH = 6.40 is 0.008 ± 0.004 ppm. Figure 7 shows the residue-specific differences between MES and phosphate-buffered samples. Gly173 and Asn11 are both at the active site and show chemical shift changes significantly above the mean value. The other residues

dx.doi.org/10.1021/bi400973e | *Biochemistry* 2013, 52, 6548−6558

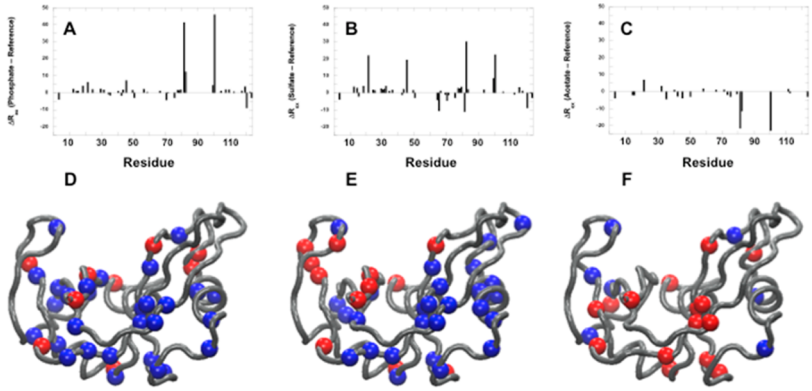

Figure 5. Solute-dependent R_{ex} changes. Differences in R_{ex} between MES-reference and phosphate (A), sulfate (B), and acetate (C) containing RNase A samples as a function of amino acid sequence. In (D) and (E), the changes (positive, blue and negative, red) are shown as spheres on the respective backbone trace of RNase A. Data is only shown in (A)−(F) in which the difference in R_{ex} value is > than 20% of the MES-reference sample.

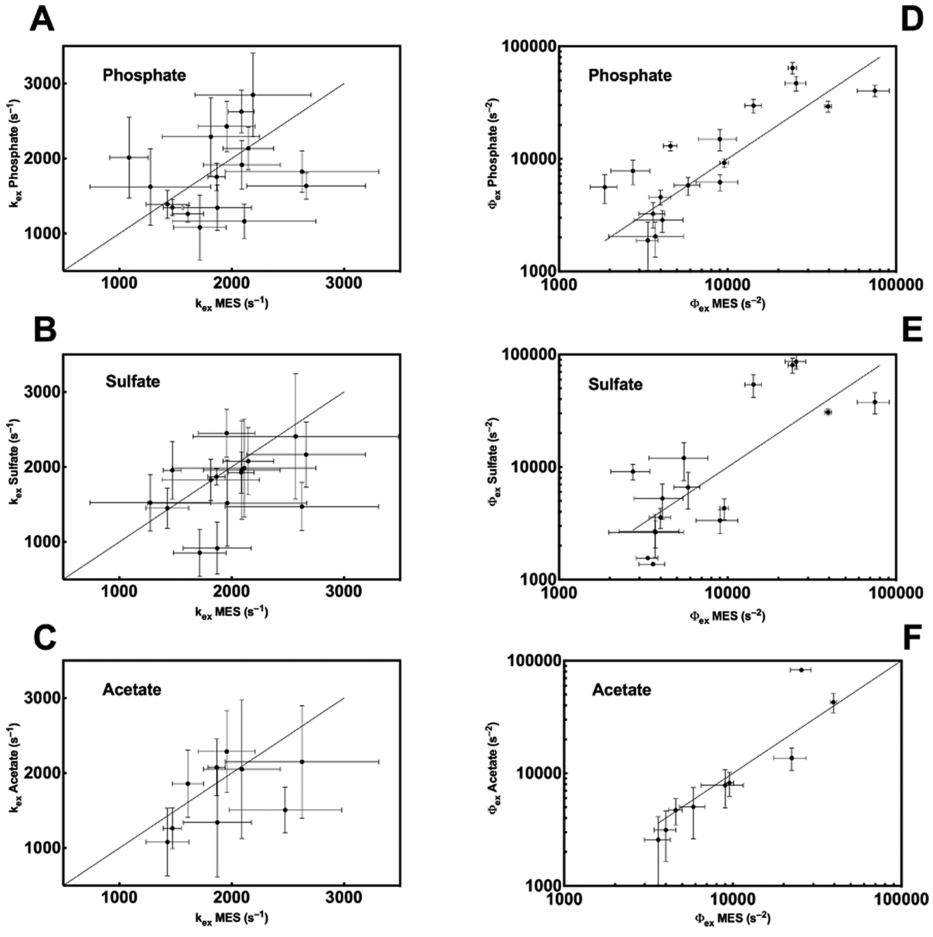

Figure 6. Comparison of conformational exchange parameters. A comparison of exchange rate constants (k_{ex}) from the MES reference is given in (A)−(C) for phosphate, sulfate, and acetate, respectively. ϕ_{ex} comparisons are shown for the same samples in (D)−(F). All data were obtained at 600 MHz from fits to eq 1. The diagonal lines in each have a slope of 1 to indicate a perfect correlation between the data points. In (D)−(F), the axes are shown in a $\log_{10}$ scale for viewing purposes only.

with Δ > 0.02 ppm (Thr27, Ile92, Thr139, Glu145, Ala201, His224, and Val226) are located throughout the TIM structure (Figure 7B).

R_2 values for TIM differ site-specifically depending on the buffer, with many residues experiencing an elevated transverse relaxation rate in phosphate compared to that of MES (Figure 8). The average R_2 ± standard deviation (n = 132) for phosphate-buffered TIM is 14.6 ± 3.3 s^{-1} compared to 14.7 ± 3.1 s^{-1} (n = 130) for TIM in MES buffer. The effect of buffer on conformational exchange motions in TIM was further investigated by measuring R_{ex} as shown in Figure 9.

In TIM, there are significant differences in buffer-induced changes in conformational exchange motions. R_{ex} for TIM was estimated from R_2 differences in TROSY-based CPMG

dx.doi.org/10.1021/bi400973e | Biochemistry 2013, 52, 6548−6558

Table 1. Comparison of Exchange Rate Constants from CPMG Dispersion Experiments

residue	reference k_{ex} (s^{-1})	phosphate k_{ex} (s^{-1})[a]	sulfate k_{ex} (s^{-1})[a]	acetate k_{ex} (s^{-1})[a]
Ser15	2570 ± 915	ND	2410 ± 835[b]	ND
Ser16	2570 ± 520	2850 ± 555	ND	ND
Ser22	1960 ± 250	2430 ± 335	2450 ± 320	2285 ± 545[b]
Met30	2110 ± 635	1165 ± 230	1985 ± 650[b]	ND
Val43	1275 ± 535	1625 ± 510	1524 ± 375	ND
Phe46[b]	2150 ± 225	2135 ± 285[b]	2075 ± 445	ND
Ser59	1960 ± 710	ND	1520 ± 575	ND
Ala64[b]	1430 ± 190	1390 ± 185[b]	1450 ± 270[b]	1080 ± 450
Cys65	1470 ± 80	1350 ± 110	1955 ± 385	1265 ± 270
Lys66	2665 ± 530	1635 ± 175	2165 ± 435	ND
Asn67	1085 ± 170	2015 ± 540	ND	ND
Thr70	2625 ± 680	1825 ± 275	1470 ± 320	2150 ± 750
Asn71	1865 ± 75	1755 ± 185	1870 ± 110[b]	2075 ± 380
Gln74	1715 ± 235	1080 ± 435	855 ± 315	ND
Ser80	1815 ± 435	2290 ± 520	1830 ± 275[b]	ND
Asp83	2085 ± 115	2625 ± 285	1925 ± 275	ND
Ile106	2090 ± 340	1915 ± 325	1960 ± 660	2050 ± 925[b]
Ala109	1610 ± 140	1260 ± 110	ND	1860 ± 450
Asp121	2475 ± 500	ND	ND	1510 ± 305
Ser123	1870 ± 305	1345 ± 305	920 ± 345	1340 ± 730

[a]ND indicates no dispersion or poor fits of the data with eq 1. [b]Determined to be statistically indistinguishable from the reference sample. All other values were statistically different as determined by Monte Carlo simulations and unpaired t-tests as described in the Materials and Methods section.

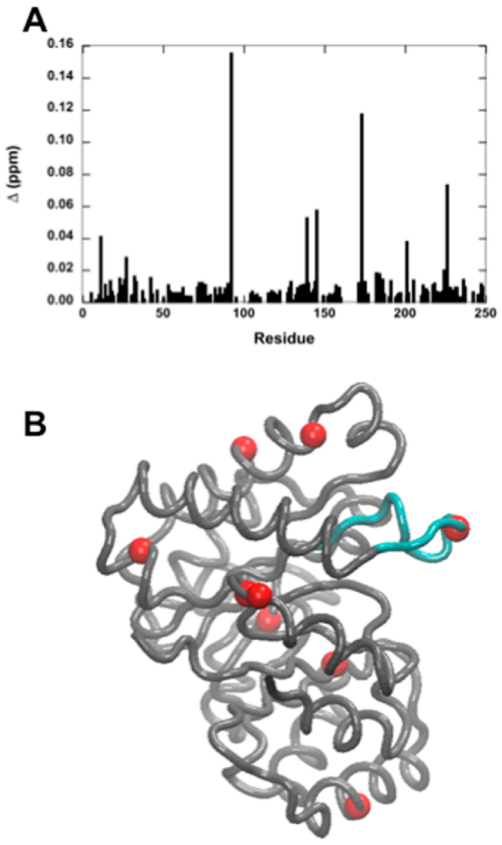

Figure 7. Buffer-altered chemical shifts in TIM. (A) Residue-specific composite chemical shift changes determined from eq 3. (B) Values of Δ > 0.02 ppm as red spheres on the TIM monomer. The active site loop 6 is cyan.

dispersion experiments using τ_{cp} = 0.625 and 10 ms with total relaxation delay = 40 ms. The R_{ex} value estimated from the differences in R_2 at the long and short of τ_{cp} values represents a

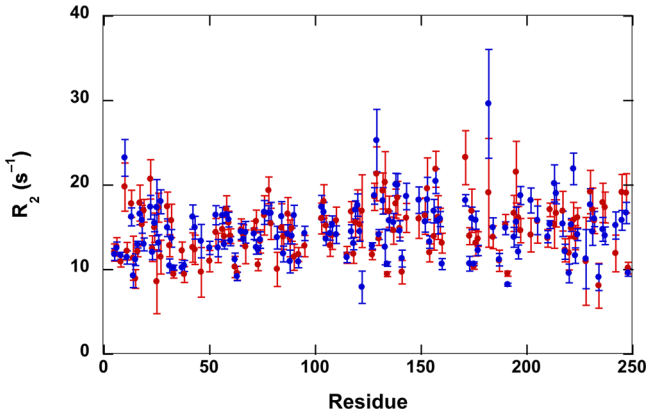

Figure 8. Transverse relaxation rates for V167P/W168E TIM in MES (red) and phosphate (blue) buffers. Relaxation rates were determined using the two point method with τ_{cp} = 0.625 and 0.0 ms in a TROSY-relaxation compensated CPMG experiment at a total relaxation delay of 20 ms. Uncertainties were determined from duplicate experiments.

lower limit to R_{ex}. These data are shown in Figure 9. In MES buffer (Figure 9A,C), seven residues have an R_{ex} > 3 s^{-1}. They are Lys18, Trp90, Lys141, Gln182, Arg205, Ser222, and Gly228. In phosphate buffer (Figure 9B,D), 10 residues have R_{ex} > 3 s^{-1}. One of these (Trp90) is common with the MES-buffered TIM sample. The remainder are phosphate specific: Ile46, Lys54, Ala63, Gly72, Asp85, Gly122, Glu133, Val143, and Leu220. Of particular note is the loss of millisecond motions in active site loop 6 at Gly171 in the presence of phosphate. Thus, like RNase A, TIM shows a dependence of millisecond motions on the buffer composition.

HisF. As a third example, we examined the chemical shift changes in monomeric HisF in HEPES and phosphate buffer at pH = 7.20. We had previously assigned 97% of the backbone resonances for HisF.[27] However, a comparison of HisF in HEPES and phosphate buffer shows significant chemical shift changes (Figure 10). The changes are of such magnitude that

dx.doi.org/10.1021/bi400973e | Biochemistry 2013, 52, 6548−6558

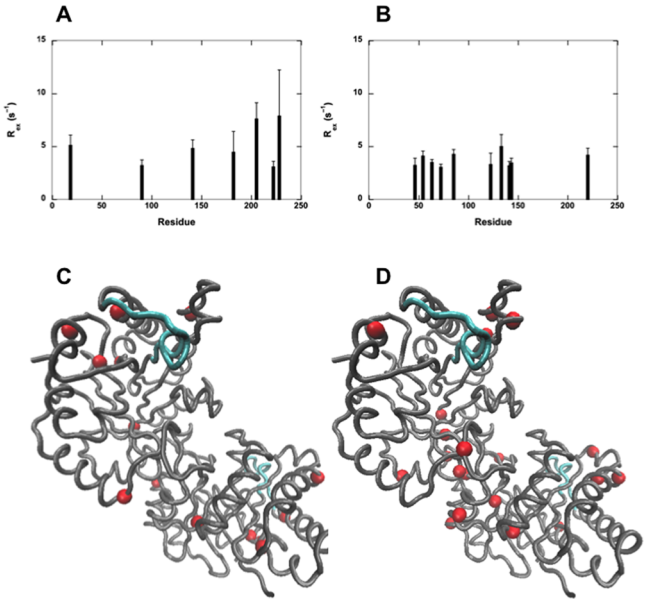

Figure 9. Conformational exchange contributions for triosephosphate isomerase dimer. (A) R_{ex} values >3 s^{-1} for MES-buffered TIM. (C) Residues indicated as red spheres on the monomer structure of the TIM dimer. (B and D) Analogous results for phosphate-buffered TIM. The active site loop 6 is cyan to orient the reader.

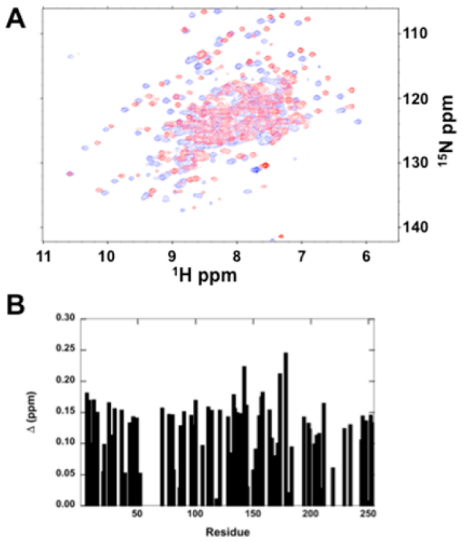

Figure 10. $^{1}H-^{15}N$ chemical shift comparison for HisF. (A) TROSY spectra for HisF in HEPES buffer (blue) and phosphate buffer (red). (B) Δ values as calculated with eq 3 for each assignable residue.

we are only able to compare 80 of the 250 NH resonances between the two buffer systems. For these 80 resonances, the protein-wide average composite shift difference (Δ) = 0.12 ± 0.05, which is over an order of magnitude larger than the average Δ value for TIM and 4-fold larger than that observed for RNase A. These large shifts suggest significant structural changes due to buffer composition. Therefore, we did not attempt to compare NMR relaxation rates because interpretation of the differences is not straightforward if larger amplitude structure changes accompany changes in millisecond motions.

DISCUSSION

The common observation of small molecule electron density in X-ray crystal structures prompted us to investigate the effect of commonly used buffer or solution additives on protein dynamics as observed by liquid-phase NMR. It is clear that phosphate, sulfate, and acetate have measurable but not dramatic effects on NMR chemical shifts for RNase A and TIM, whereas much more significant changes are observed in the HisF spectrum. Moreover, notable solute-dependent changes in conformational motions for RNase A and TIM were observed through their effects on transverse relaxation rate constants. The observed changes in ^{15}N R_2 values are not due to changes in RNase A and TIM aggregation state, which are monomeric in the case of RNase A and dimeric for TIM. For RNase A, the overall R_2 values are the same no matter the solute, indicating that the overall rotational correlation times are the same. Second, we are working at [RNase A] < 800 μM, a concentration that we previously determined to be the upper limit for fully monomeric RNase A. Likewise for TIM, previous NMR studies indicate that it does not aggregate up to concentrations of 2 mM. For HisF, despite the large chemical shift changes, the protein-wide average amide ^{15}N linewidths are similar in HEPES (32 ± 8 Hz) and phosphate (31 ± 10 Hz), indicating no significant alteration in aggregation state. The observed changes in millisecond motions and chemical shifts thus appear to be due to direct binding of the solute to RNase A, TIM, and HisF.

Binding of the small solute molecules to these three enzymes is not surprising. The function of RNase A is to bind polyanionic RNA; therefore, RNase A is highly positively charged at its active site (Figure 11A). Phosphate is a known RNase A inhibitor. Published values for the dissociation constant of the enzyme−inhibitor complex give K_I = 2−15 mM for phosphate, with similar values for sulfate and acetate.[13] Under the conditions of these experiments, these anionic buffers occupy the active site at approximately 85%−95% saturation, but as discussed below, active site binding only accounts for some of the buffer−RNase A interactions. Phosphate is observed to bind at the RNase A active site, near Lys41, His12, His119, and Gln11 in the crystal structure 5RSA, despite being present in the crystallographic solution at modest (10 mM) concentrations (Figure 11B).[34] The majority of observed chemical shift changes occur at the active site, yet the changes in millisecond motions occur throughout the enzyme. It seems likely that the multiple phosphate binding sites used for substrate (P1′, P0, P1, P2) might also be involved in binding inorganic phosphate and subsequently altering the millisecond motions throughout the enzyme, resulting in changes in the relaxation dispersion curves. Given this weak binding, we are not able to determine if the changes in dispersion curves are due to changes in intramolecular motions or are the result of a bimolecular chemical exchange process between free and bound enzyme that confounds the inherent protein motions.

Multiple sulfate binding sites have also been suggested from the Raman spectra of RNase A obtained by Chen and Lord in 1976.[35] Like phosphate, a sulfate ion is observed at the active site of RNase A in the X-ray structure 1RN3 (Figure 11C).[36] Thus, the altered chemical shifts and protein motions are likely the result of several sulfate molecules interacting with RNase A. Residues that lose dispersion are localized either in loop 4 around the Ala4−sulfate hydrogen bond (Ala4, Lys66, Thr70,

dx.doi.org/10.1021/bi400973e | *Biochemistry* 2013, 52, 6548−6558

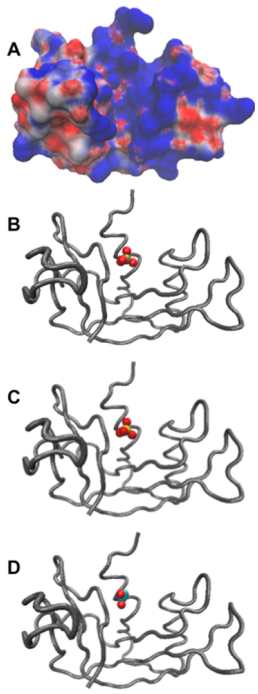

Figure 11. Crystallographic identification of ion binding sites. (A) shows an electrostatic surface rendering of RNase A viewing into the active site cleft. (B)−(D) show the same orientation as in (A) with phosphate (B), sulfate (C), and acetate (D) bound near the P1 site. The electrostatic surface was generated with the APBS[37] and VMD.[38] The structures used for (B)−(D) are 5RSA, [34] 1RN3,[36] and 4RSD, respectively.[39]

Asn71, Ala109) or near the sulfate-binding residues Lys41 and Val43. In confirmation of the suggested role of Ala4, this residue displays the largest change in R_{ex} relative to the reference (reference:sulfate R_{ex} ratio 9.5 ± 5.3 s^{-1}, versus 1.7 ± 0.40 s^{-1} for Val43, 1.6 ± 0.18 s^{-1} for Lys66, 1.5 ± 0.22 s^{-1} for Thr70, 1.3 ± 0.04 s^{-1} for Asn71, and 3.6 ± 0.21 s^{-1} for Ala109). Residues that gain dispersion are localized around loop 1 near His48 (Ser15, Ala19, Thr78) or at the active site (Asp83). The approximate amount of gain in R_{ex} was constant across the group (sulfate:reference R_{ex} ratio 2.3 ± 0.45 s^{-1} for Ser15, 5.5 ± 1.5 s^{-1} for Ala19, 3.1 ± 1.0 s^{-1} for Thr78, and 3.6 ± 0.21 s^{-1} for Asp83).

As reported above, sulfate had the highest stabilization effect against urea denaturation.[13] At concentrations of 80 mM, sulfate shifts the pK_a values of the active site residues His12 and His119 by ∼0.4; the anion does not perturb His48.[15] Sulfate binds the P1 site and hydrogen bonds to Ala4 as SO_4, which also interacts with α helix dipole moments; the bound anion facilitates conversion of His119 from the A to the B conformation.[16] As discussed above, Berisio et al. observe that neutral pH results in release of a sulfate ion from the active site (where the anion is bound to His12, His119, and Lys41), which in turn mediates conformational changes in Lys41 and Gln11. The anion release is thought to correlate with pH-driven changes in electrostatic potential, and Lys7, Arg10, Arg39, and Lys66 constitute the main contributors to loss of Lys41−sulfate binding interaction.[14]

Acetate is quite commonly used as an NMR buffer because deuterated acetate is relatively inexpensive; in addition, its pK_a is <6 and therefore its buffer capacity resides in an NMR-desirable range that minimizes amide proton exchange. However, it has long been known that acetate alters the functionally important millisecond motions in RNase A. Markley,[40] and later Loria and co-workers,[8,10,12] showed that His48 is a critical player in the motion of loop 1 and therefore is the rate-limiting product release step. The participation of His48 in this conformational change was identified by a discontinuity in the pH titration profile for His48. It was demonstrated earlier that acetate-binding transforms the pH titration of His48 such that it exhibits "normal" pH-induced shifts, suggesting a change in motion to one slower than the chemical shift time scale.[41,42] Thus, acetate binds to the RNase A active site and alters the time scale of motion for a critical loop in this enzyme, suggesting that acetate appears to induce long-range changes in conformational motions.

The binding interactions of acetate are comparable to those of phosphate (Figure 11D). Markley noted that 0.2 M acetate effectively converted the discontinuous pH titration of RNase A to one that resembled that of RNase S (a proteolyzed RNase A), suggesting altered backbone hydrogen bonds between His12−Val47, Asp14−Val47, Ser16−His48, Ser16−Ala20, and Ser50−Val54 and a conformational change that shifts the side chain of His48 further from the ring of Tyr25.[40] At 0.1 M concentration, acetate causes a 42 ± 2% stabilization of RNase A against urea denaturation.[13]

For these three buffer components, the changes in observed millisecond motions are not due to large structural changes but rather alterations in conformational motions. First, X-ray crystal structures of phosphate-bound, sulfate-bound, and acetate-bound show backbone rmsd with ligand-free RNase A of 0.123, 0.308, and 0.369 Å, respectively. Second, we calculated the ^{15}N chemical shifts for these four crystal structures using ShiftX2[43] and compared those shifts with measured ^{15}N shifts. There is a high degree of correlation between calculated ^{15}N chemical shifts for each RNase A structure with the measured chemical shifts (Supporting Information Figure S3). For ligand-free, phosphate-bound, sulfate-bound, and acetate-bound R^2 values are 0.95, 0.91, 0.91, and 0.93, respectively, with slopes equal to 1 in all cases. Thus, the measured chemical shifts are a good indication that the overall structure of RNase A is not changing significantly. The outlier residues noted in Supporting Information Figure S3 are located at the anion binding sites; therefore, the deviation from calculated shifts is likely due to specific interaction with the anionic ligands.

These buffer-altered millisecond motions are not specific to RNase A. Triosephosphate isomerase also exhibits changes in millisecond motions in MES buffer compared to that of phosphate. It is important to note that these studies were done on the identical enzyme sample in which the buffer exchange was done by dialysis. In TIM, some of the altered motions occur at the active site and result in an observed loss of motions in the active site loop 6. The N^H of Gly171 makes interactions with the phosphate moiety of the substrate at the active site when loop 6 is closed. The different motions observed for these two residues suggest that phosphate is likely causing loop 6 to increasingly populate the closed loop 6 conformation compared to the MES sample. However, the pattern of chemical shift changes does not resemble those observed when the substrate analog, glycerol-3-phosphate, is bound to TIM at the active site.[44] Thus, although it is reasonable to expect that some of the changes in motions and chemical shifts are due to phosphate binding at the active site, the other alterations in motions and chemical shifts are likely due to weak binding at locations distant from the active site.

HisF is the 253 amino acid cyclase subunit of imidazole glycerol phosphate synthase (IGPS). It is stable in isolation from its glutaminase (HisH) partner, and the crystal structure of HisF has been solved.[45] In its monomeric form, HisF retains the ability to bind its substrate molecules. When switching from HEPES to phosphate buffer, there are widespread amide chemical shift changes that are of significant magnitude. These changes in amide shifts are similar in magnitude to those observed when the product of the IGPS reaction, imidazole glycerol phosphate (IGP), binds to the enzyme.[46] These large changes in shifts are perhaps not surprising because phosphate is a competitive inhibitor with respect to the substrate PRFAR and is observed at the HisF active site in crystal structures, where it is believed that the two bound phosphates are located at the two phosphate sites that are normally occupied by the phosphate groups on the substrate PRFAR.[45] Thus, in HisF, unlike RNase A and TIM, the main contributions to the chemical shift changes are likely active site specific and result in protein-wide conformational changes.

The data presented here clearly show that millisecond motions can be altered by commonly used solutes either by conformational changes or by intermolecular exchange. These results are likely not restricted to those buffers studied here, as it is known that chloride and formate also bind to the RNase A active site and sulfate binds to the TIM active site. The results presented above are specific to the three enzymes studied, but the somewhat general electrostatic protein−ligand interactions these ions make with those enzymes suggests that they could behave in similar fashion with other enzymes whose function is to bind anionic substrates at either the active site or a known (or unknown) allosteric site. In general, other commonly used "buffers or additives" such as DTT, β-mercaptoethanol, NH_4^+, EDTA, TRIS, glycerol, citrate, or azide could also result in alteration or abrogation of the true protein dynamics; these effects may or may not be predictable, a priori, and will certainly be protein-dependent. A query of the PDB and NMR data bank (BioMagResBank) shows that the small molecules listed above are used in thousands of NMR experiments. That these millisecond motions in RNase A, TIM, and HisF have been previously identified as important in catalytic or allosteric function suggests great care must be taken when deciding on solution conditions for one's biophysical studies. The data in this work indicates that an incorrect choice of buffer or additive can result in the masking of important motions and, moreover, in the observation of apparent motions that are due to buffer binding but which could be misinterpreted as functionally relevant in the absence of other data.

An obvious question is what buffer should be used in such NMR studies. Although this will certainly be protein-dependent, an excellent guideline remains the work published by Good et al in 1966.[47] Summarizing that work, phosphate is best avoided because many metabolites contain phosphate and it tends to form complexes with other cations. Likewise, the reactivity of primary amines suggests that Tris buffer should also not be used. Thus, the recommendation of that work stands: zwitterionic buffers such as MES, HEPES, PIPES, and so forth are the least likely to interact with one's biological macromolecule, they have good buffering capacity, and importantly, they possess a relatively small $\Delta pK_a/°C$, which is essential for temperature-dependent studies.

■ ASSOCIATED CONTENT

Ⓢ Supporting Information

CPMG dispersion curves for all residues, exempting those with incomplete data sets due to ambiguous peak assignments. This material is available free of charge via the Internet at http://pubs.acs.org.

■ AUTHOR INFORMATION

Corresponding Author

*J. P. Loria. E-mail: patrick.loria@yale.edu. Phone: 203-436-2518.

Present Address

[§]Department of Chemistry, Massachusetts Institute of Technology, Cambridge, Massachusetts.

Funding Sources

J.P.L acknowledges funding from the National Science Foundation (MCB-0744161). G.K. was supported in part by an NIH biophysics training grant (T32GM008283).

Notes

The authors declare no competing financial interest.

■ ACKNOWLEDGMENTS

This work was performed by M.W. as part of the Yale University requirements for a B.Sc. degree in Chemistry.

■ ABBREVIATIONS

HEPES, 2-[4-(2-hydroxyethyl)piperazin-1-yl]ethanesulfonic acid; MES, 2-(*N*-morpholino)ethanesulfonic acid; RNase A, bovine pancreatic ribonuclease A; CPMG, Carr−Purcell−Meiboom−Gill

■ REFERENCES

(1) Mann, P. J., and Woolf, B. (1930) The action of salts on fumarase. I. *Biochem. J. 24*, 427−434.

(2) Alberty, R. A., Massey, V., Frieden, C., and Fuhlbrigge, A. R. (1954) Studies of the enzyme fumarase: III. The dependence of the kinetic constants at 25° upon the concentration and pH of phosphate buffers. *J. Am. Chem. Soc. 76*, 2485−2493.

(3) Massey, V. (1953) Studies on fumarase. II. The effects of inorganic anions on fumarase activity. *Biochem. J. 53*, 67−71.

(4) Mahler, H. R. (1961) The use of amine buffers in studies with enzymes. *Ann. N. Y. Acad. Sci. 92*, 426−439.

(5) Pegan, S. D., Rukseree, K., Capodagli, G. C., Baker, E. A., Krasnykh, O., Franzblau, S. G., and Mesecar, A. D. (2013) Active site loop dynamics of a class IIa fructose 1,6-bisphosphate aldolase from Mycobacterium tuberculosis. *Biochemistry 52*, 912−925.

(6) Beach, H., Cole, R., Gill, M. L., and Loria, J. P. (2005) Conservation of μs-ms enzyme motions in the apo- and substrate-mimicked state. *J. Am. Chem. Soc. 127*, 9167−9176.

(7) Cole, R., and Loria, J. P. (2002) Evidence for flexibility in the function of ribonuclease A. *Biochemistry 41*, 6072−6081.

(8) Doucet, N., Watt, E. D., and Loria, J. P. (2009) The flexibility of a distant loop modulates active site motion and product release in ribonuclease A. *Biochemistry 48*, 7160−7168.

(9) Kovrigin, E. L., and Loria, J. P. (2006) Enzyme dynamics along the reaction coordinate: critical role of a conserved residue. *Biochemistry 45*, 2636−2647.

(10) Kovrigin, E. L., and Loria, J. P. (2006) Characterization of the transition state of functional enzyme dynamics. *J. Am. Chem. Soc. 128*, 7724−7725.

(11) Watt, E. D., Rivalta, I., Whittier, S. K., Batista, V. S., and Loria, J. P. (2011) Reengineering rate-limiting, millisecond enzyme motions by introduction of an unnatural amino acid. *Biophys. J. 101*, 411−420.

(12) Watt, E. D., Shimada, H., Kovrigin, E. L., and Loria, J. P. (2007) The mechanism of rate-limiting motions in enzyme function. *Proc. Natl. Acad. Sci. U. S. A. 104*, 11981−11986.
(13) Nelson, C. A., Hummel, J. P., Swenson, C. A., and Friedman, L. (1962) Stabilization of pancreatic ribonuclease against urea denaturation by anion binding. *J. Biol. Chem. 237*, 1575−1580.
(14) Berisio, R., Sica, F., Lamzin, V. S., Wilson, K. S., Zagari, A., and Mazzarella, L. (2002) Atomic resolution structures of ribonuclease A at six pH values. *Acta Crystallogr., Sect. D: Biol. Crystallogr. 58*, 441−450.
(15) Meadows, D. H., Roberts, G. C., and Jardetzky, O. (1969) Nuclear magnetic resonance studies of the structure and binding sites of enzymes. 8. Inhibitor binding to ribonuclease. *J. Mol. Biol. 45*, 491−511.
(16) Fedorov, A. A., Joseph-McCarthy, D., Fedorov, E., Sirakova, D., Graf, I., and Almo, S. C. (1996) Ionic interactions in crystalline bovine pancreatic ribonuclease A. *Biochemistry 35*, 15962−15979.
(17) Mueller-Dieckmann, C., Panjikar, S., Schmidt, A., Mueller, S., Kuper, J., Geerlof, A., Wilmanns, M., Singh, R. K., Tucker, P. A., and Weiss, M. S. (2007) On the routine use of soft X-rays in macromolecular crystallography. Part IV. Efficient determination of anomalous substructures in biomacromolecules using longer X-ray wavelengths. *Acta Crystallogr., Sect. D: Biol. Crystallogr. 63*, 366−380.
(18) Joseph, D., Petsko, G. A., and Karplus, M. (1990) Anatomy of a conformational change: Hinged "lid" motion of the triosephosphate isomerase loop. *Science 249*, 1425−1428.
(19) Berlow, R. B., Igumenova, T. I., and Loria, J. P. (2007) Value of a hydrogen bond in triosephosphate isomerase loop motion. *Biochemistry 46*, 6001−6010.
(20) Derreumaux, P., and Schlick, T. (1998) The loop opening/closing motion of the enzyme triosephosphate isomerase. *Biophys. J. 74*, 72−81.
(21) Massi, F., Wang, C., and Palmer, A. G., 3rd (2006) Solution NMR and computer simulation studies of active site loop motion in triosephosphate isomerase. *Biochemistry 45*, 10787−10794.
(22) Rozovsky, S., Jogl, G., Tong, L., and McDermott, A. E. (2001) Solution-state NMR investigations of triosephosphate isomerase active site loop motion: ligand release in relation to active site loop dynamics. *J. Mol. Biol. 310*, 271−280.
(23) Williams, J. C., and McDermott, A. E. (1995) Dynamics of the flexible loop of triosephosphate isomerase: the loop motion is not ligand gated. *Biochemistry 34*, 8309−8319.
(24) Loria, J. P., Rance, M., and Palmer, A. G. (1999) A Relaxation-compensated Carr-Purcell-Meiboom-Gill sequence for characterizing chemical exchange by NMR spectroscopy. *J. Am. Chem. Soc. 121*, 2331−2332.
(25) Loria, J. P., Rance, M., and Palmer, A. G. (1999) A TROSY CPMG sequence for characterizing chemical exchange in large proteins. *J. Biomol. NMR 15*, 151−155.
(26) Kempf, J. G., Jung, J. Y., Ragain, C., Sampson, N. S., and Loria, J. P. (2007) Dynamic requirements for a functional protein hinge. *J. Mol. Biol. 368*, 131−149.
(27) Lipchock, J. M., and Loria, J. P. (2008) 1H, 15N and 13C resonance assignment of imidazole glycerol phosphate (IGP) synthase protein HisF from Thermotoga maritima. *Biomol. NMR Assignments 2*, 219−221.
(28) Luz, Z., and Meiboom, S. (1963) Nuclear magnetic resonance study of the protolysis of trimethylammonium ion in aqueous solution—order of the reaction with respect to solvent. *J. Chem. Phys. 39*, 366−370.
(29) Mulder, F. A., Skrynnikov, N. R., Hon, B., Dahlquist, F. W., and Kay, L. E. (2001) Measurement of slow (micros-ms) time scale dynamics in protein side chains by (15)N relaxation dispersion NMR spectroscopy: application to Asn and Gln residues in a cavity mutant of T4 lysozyme. *J. Am. Chem. Soc. 123*, 967−975.
(30) Grzesiek, S., Stahl, S. J., Wingfield, P. T., and Bax, A. (1996) The CD4 determinant for downregulation by HIV-1 Nef directly binds to Nef. Mapping of the Nef binding surface by NMR. *Biochemistry 35*, 10256−10261.
(31) Doucet, N., Jayasundera, T. B., Simonovic, M., and Loria, J. P. (2010) The crystal structure of ribonuclease A in complex with thymidine-3′-monophosphate provides further insight into ligand binding. *Proteins 78*, 2459−2468.
(32) Kovrigin, E. L., Cole, R., and Loria, J. P. (2003) Temperature dependence of the backbone dynamics of Ribonuclease A in the ground state and bound to the inhibitor 5′-phosphothymidine (3′-5′) pyrophosphate adenosine 3′-phosphate. *Biochemistry 42*, 5279−5291.
(33) Raines, R. T. (1998) Ribonuclease A. *Chem. Rev. 98*, 1045−1066.
(34) Wlodawer, A., Bott, R., and Sjolin, L. (1982) The refined crystal structure of ribonuclease A at 2.0 A resolution. *J. Biol. Chem. 257*, 1325−1332.
(35) Chen, M. C., and Lord, R. C. (1976) Laser Raman spectroscopic studies of the thermal unfolding of ribonuclease A. *Biochemistry 15*, 1889−1897.
(36) Borkakoti, N., Moss, D. S., and Palmer, R. A. (1982) Ribonuclease-A. Least-squares refinement of the structure at 1.45 Angstroms resolution. *Acta Crystallogr., Sect. B: Struct. Crystallogr. Cryst. Chem. 38*, 2210.
(37) Baker, N. A., Sept, D., Joseph, S., Holst, M. J., and McCammon, J. A. (2001) Electrostatics of nanosystems: application to microtubules and the ribosome. *Proc. Natl. Acad. Sci. U. S. A. 98*, 10037−10041.
(38) Humphrey, W., Dalke, A., and Schulten, K. (1996) VMD: visual molecular dynamics. *J. Mol. Graphics 14* (33−38), 27−38.
(39) Schultz, L. W., Quirk, D. J., and Raines, R. T. (1998) His...Asp catalytic dyad of ribonuclease A: structure and function of the wild-type, D121N, and D121A enzymes. *Biochemistry 37*, 8886−8898.
(40) Markley, J. L. (1975) Correlation proton magnetic resonance studies at 250 MHz of bovine pancreatic ribonuclease. II. pH and inhibitor-induced conformational transitions affecting histidine-48 and one tyrosine residue of ribonuclease A. *Biochemistry 14*, 3554−3561.
(41) Meadows, D. H., Markley, J. L., Cohen, J. S., and Jardetzky, O. (1967) Nuclear magnetic resonance studies of the structure and binding sites of enzymes. I. Histidine residues. *Proc. Natl. Acad. Sci. U. S. A. 58*, 1307−1313.
(42) Tanokura, M. (1983) 1H nuclear magnetic resonance titration curves and microenvironments of aromatic residues in bovine pancreatic ribonuclease A. *J. Biochem. 94*, 51−62.
(43) Han, B., Liu, Y., Ginzinger, S. W., and Wishart, D. S. (2011) SHIFTX2: significantly improved protein chemical shift prediction. *J. Biomol. NMR 50*, 43−57.
(44) Wang, Y. (2010) Ph.D. Thesis, Yale University, New Haven, CT.
(45) Lang, D., Thoma, R., Henn-Sax, M., Sterner, R., and Wilmanns, M. (2000) Structural evidence for evolution of the beta/alpha barrel scaffold by gene duplication and fusion. *Science 289*, 1546−1550.
(46) Lipchock, J., and Loria, J. P. (2009) Millisecond dynamics in the allosteric enzyme imidazole glycerol phosphate synthase (IGPS) from Thermotoga maritima. *J. Biomol. NMR 45*, 73−84.
(47) Good, N. E., Wingnet, D., Winter, W., Connolly, T. N., Izawa, S., and Singh, R. M. M. (1966) Hydrogen ion buffers for biological research. *Biochemistry 5*, 467−477.